Long-Term Datasets for the Understanding
of Solar and Stellar Magnetic Cycles
Proceedings IAU Symposium No. 340, 2018
D. Banerjee, J. Jiang, K. Kusano & S. Solanki, eds.

doi:10.1017/S1743921318001060

Turbulent diffusion in the photosphere as observational constraint on dynamo theories

Valentina I. Abramenko

Crimean Astrophysical Observatory, p/o Nauchny, Crimea, 298409, Russia
email: vabramenko@gmail.com

Abstract. We utilized line-of-sight magnetograms acquired by HMI/SDO to derive the value of turbulent magnetic diffusivity in undisturbed photosphere. Two areas, a coronal hole area (CH) and an area a super-granulation pattern, SG, were analyzed. The behavior of the turbulent diffusion coefficient on time scales of 1000-40000 s and spatial scales of 500-6000 km was explored. Small magnetic elements in both CH and SG areas disperse in the same way and they are more mobile than the large elements. The regime of super-diffusivity is found for small elements (the turbulent diffusion coefficient K growths from 100 to 300 km^2 s^{-1}). Large magnetic elements disperse differently in the CH and SG areas. Comparison of these results with the previously published shows that there is a tendency of saturation of the diffusion coefficient on large scales, i.e., the turbulent regime of super-diffusivity gradually ceases so that normal diffusion with a constant value of $K \approx 500$ km^2 s^{-1} might be observed on time scales longer than a day. The results show that the turbulent diffusivity should not be considered in modeling as a scalar, the flux- and scale-dependence is obvious.

Keywords. Sun: magnetic fields, Sun: photosphere, Sun: fundamental parameters, methods: data analysis

1. Introduction

One of the key parameters of these flux transport models - the value of turbulent magnetic diffusivity - is the most poorly constrained both theoretically and observationally. However, the relationship between turbulent diffusion and advection (caused by meridional circulation and differential rotation) determines the solar cycle memory and thus affects the prediction of an oncoming cycle (Yeates *et al.* 2008). The flux transport models make use of various profiles of the turbulent diffusivity in the convective zone, however usually the models adopt a constant value of the diffusion coefficient on the solar surface, which substantially changes from one model to another: from 5 km^2 s^{-1} (Jouve & Brun 2007) to 600 km^2 s^{-1} (Jiang *et al.* 2010). Solar observations, as interpreted in the framework of normal diffusion, always produce values below 300-350 km^2 s^{-1} (see, e.g., Utz *et al.* 2010). Moreover, observational estimates strongly depend on the characteristic spatial and temporal scales of utilized data. The magnitude of the magnetic turbulent diffusivity derived from observations, as well as the scale dependence of the magnetic diffusion coefficient is needed to calibrate the diffusivity profiles in theoretical dynamo models (Dikpati & Charbonneau 1999, Jouve *et al.* 2008). To clarify the issue, the seeing-free non-stop data acquired by the Helioseismic and Magnetic Imager (HMI) onboard the Solar Dynamic Observatory (SDO, Scherrer *et al.* 2012) were utilized for a weakest magnetic environment, a coronal hole, and for a typical supergranula pattern.

2. Method and Data Processing

The commonly accepted mechanism for transporting the magnetic flux over the solar surface on small scales is random walk, or, normal diffusion, when the mean-squared displacement of flow tracers varies with time, τ, as $\langle(\Delta l)^2\rangle = 4K\tau \sim \tau^{\gamma}$, where K is the diffusion coefficient (a scalar), and $\gamma = 1$, e.g., Monin & Yaglom (1975). Generally, when index γ deviates from unity, diffusion is called anomalous diffusion. A regime with $\gamma > 1$ is called super-diffusive, while $\gamma < 1$, indicates sub-diffusive. Parameters $\langle(\Delta l)^2\rangle$ and γ, generally derived from observations, allow us to determine the diffusion coefficient as a function of time and spatial scales (Abramenko *et al.* 2011). Recent researches based on the new-generation of solar instrumentation (Abramenko *et al.* 2011, Giannattasio *et al.* 2014, Jafarzadeh *et al.* 2017) suggest that on smallest observable scales the diffusion coefficient is not constant and varies in direct proportion to the spatial and time scales suggesting the turbulent regime of super-diffusivity in the photosphere.

To obtain the values $\langle(\Delta l)^2\rangle$, usually the displacements of individual tracers are calculated, and the spectrum $\langle(\Delta l)^2\rangle$ versus τ is called as displacement spectrum (e.g., Abramenko *et al.* 2011). To reduce the influence of advection and estimate the turbulent diffusivity, the pair separation spectrum (Monin & Yaglom 1975) can be applied. Here, distances between two tracers at consecutive moments are calculated. Since large-scale advection is expected to effect both tracers equally, it is eliminated (Lepreti *et al.* 2012). A comparison between the displacement and separation spectra can provide information on the properties of the dispersal mechanism.

The two data sets considered in this study consist of magnetogram series obtained with SDO/HMI instrument. The line-of-sight hmi.M-720s magnetograms of 12 minutes cadence were analyzed. Two regions of interest were selected: an area inside a low-latitude coronal hole (hereinafter CH-area) which crossed the central meridian on January 3, 2016 at approximately 17:12 UT, and an area of decayed active region remains, a typical supergranula pattern (hereinafter SG-area) culminated around December 1, 2015 at 8:36 UT. The size of the CH-area was restricted by the boundaries of the coronal hole and consisted approximately 230×230 Mm. The SG-area covered 275×286 Mm. Each data set of 240 magnetograms was carefully aligned using a sub-pixel alignment code based on the fast Fourier transform.

To detect magnetic elements and calculate their trajectories, we applied the modified feature detection and tracking code elaborated in Abramenko *et al.* (2011) for tracking photospheric magnetic bright points. In this study, we used the absolute value of the magnetic field as input. The thresholding technique was applied to obtain a mask of magnetic elements. To count the weakest observed elements and at the same time to mitigate an influence of noise, we choose the threshold of $th = 20$ Mx sm^{-2}, which corresponds to the triple noise level. A range of sizes of detected elements was selected between 3 and 100 square pixels.

As for the coronal hole area, the above procedure results in Set 1 data, i.e., small magnetic elements trajectories inside the CH area. To explore dispersion of large magnetic elements, higher values of the threshold and size were selected. Our experience shows that the best choice to detect magnetic elements forming the super-granula boundaries, i.e., network (NW) ensemble, is the threshold of 130 Mx sm^{-2} and the size range of 20-400 square pixels. For the CH area, this procedure gives us the Set 2 data.

Correspondingly, for the SG-area of well-pronounced network pattern, we obtained Set 3 for small elements and Set 4 for large elements. The later represents the majority of the network elements nested on the boundaries of super-granules.

https://doi.org/10.1017/S1743921318001060 Published online by Cambridge University Press

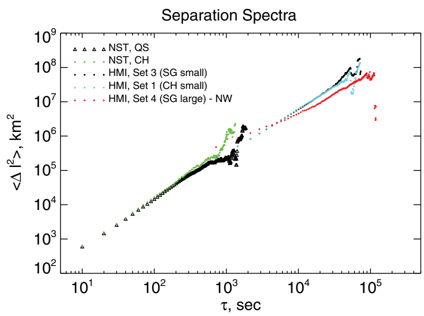

Figure 1. Separation spectra obtained using the data from different instruments. Triangles and green circles denote the NST/BBSO results for quiet sun and coronal hole regions, respectively (from Lepreti *et al.* (2012)). Black and blue dots show the HMI-spectra obtained in the present study for small elements in the SG and CH areas (Sets 1 and 3), respectively, whereas the red dots represent the spectrum from large elements in the SG area (Set 4).

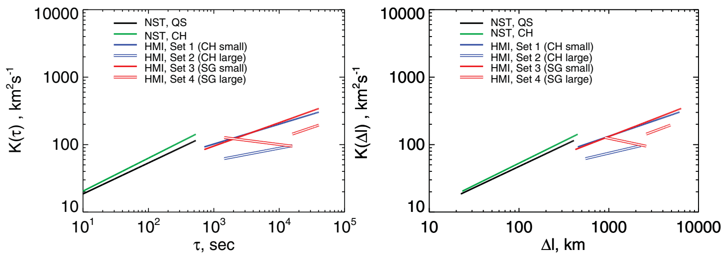

Figure 2. Left panel: diffusion coefficient as a function of temporal scale. Right panel: diffusion coefficient as a function of spatial scale.

To calculate the spectra, a method elaborated in Abramenko *et al.* (2011), Lepreti *et al.* (2012) was utilized. The method allows to obtain the turbulent diffusivity coefficient, K, as a function of temporal and spatial scales:

$$K(\tau) = \frac{c\gamma}{4}\tau^{\gamma-1}, \tag{2.1}$$

$$K(\Delta l) = \frac{c\gamma}{4}((\Delta l)^2/c)^{(\gamma-1)/\gamma}, \tag{2.2}$$

where value of γ and c are derived from the best linear fit to the spectral data points plotted in a double-logarithmic plot.

3. Results and conclusions

We found that for all analyzed data sets, the displacement and corresponding separation spectra are very close to each other. This implies that on time scales below $4 \cdot 10^4$ s, or ∼11 hours and spatial scales below ∼ 6 Mm, large-scale, quasi-regular patterns of the photospheric horizontal velocity field (advection) do not affect the magnetic flux dispersion.

In Figure 1 the separation spectra obtained in this study are overplotted with the previously published data. A general tendency is well pronounced: The spectrum becomes more shallow as the scale increases, i.e., the index γ reduces and the regime of well-developed super-diffusivity tends to become closer to the normal diffusion on larger scales.

The diffusion coefficients as derived from the separation spectra are presented in Figure 2 along with the similar data from the NST-observations reported by Lepreti *et al.*

https://doi.org/10.1017/S1743921318001060 Published online by Cambridge University Press

(2012). The coefficient increases with scales for all data sets (except Set 4), however, the growth rate becomes slower on larger scales. A fair agreement between tiny magnetic bright points (NST data set) and small HMI-magnetic elements (Sets 1 and 3) is noticeable. However, large magnetic elements (Sets 2 and 4, double lines in Fig. 2) demonstrate the significantly lower values of K, which implies the suppressed flux dispersion inside the supergranula boundaries relative to the intergranular zones.

Summarizing, we can conclude:

- Displacement and separation spectra are very similar to each other for all analyzed data sets, which allows us to suggest that possible influence of large-scale velocity patterns is negligible for the magnetic flux dispersion on scales of interest and, therefore, the inertial range turbulence is explored.

- Small magnetic elements in both CH and SG areas disperse in the same way and they are more mobile than the large ones. The regime of super-diffusivity is found for them ($\gamma \approx 1.3$ and K growths from ∼100 to ∼300 km^2 s^{-1}).

- Large magnetic elements in both CH and SG areas disperse slower than the small elements. In the CH area they are scanty and show super-diffusion with $\gamma \approx 1.2$ and $K_s = (62 - 96)$ km^2 s^{-1} on rather narrow scale range of 500-2200 km. Large elements of the SG area demonstrate a band in the spectra and, as a consequence, two ranges of linearity and two diffusivity regimes: the sub-diffusivity on scales (900-2500) km with $\gamma = 0.88$ and K decreasing from ∼130 to ∼100 km^2 s^{-1}, and the super-diffusivity on scales (2500-4800) km with $\gamma \approx 1.3$ and K growing from ∼140 to ∼200 km^2 s^{-1}.

Comparison of our results with the previously published shows that there is a tendency of saturation of the diffusion coefficient on large scales, i.e., the turbulent regime of super-diffusivity gradually ceases so that normal diffusion with a constant value of $K \approx 500$ km^2 s^{-1} might be observed on time scales longer than a day. We presume that only strong and large magnetic elements (capable to survive so long) can be a subject of the expected random walk.

SDO is a mission for NASA Living With a Star (LWS) program. The SDO/HMI data were provided by the Joint Science Operation Center (JSOC). The study was supported in part by the Russian Foundation for Basic Research projects 16-02-00221 and 17-02-00049.

References

Abramenko, V. I., Carbone, V., Yurchyshyn, V., and 5 coauthors, 2011, *ApJ*, 743, 133
Dikpati, M. & Charbonneau, P. 1999, *ApJ*, 518, 508
Giannattasio, F., Stangalini, M., Berrilli, F., Del Moro, D., & Bellot Rubio, L. 2014, *ApJ*, 788, 137
Jafarzadeh, S., Rutten, R. J., Solanki, S. K., and 14 coauthors, 2017, *ApJ* (Supplement Series), 229, 11
Jiang, J., Cameron, R., Schmitt, D., & Schussler, M. 2010, *ApJ*, 709, 301
Jouve, L. & Brun, A. S. 2007, *A&A*, 474, 239
Jouve, L., Brun, A. S., Arlt, R., and 9 coauthors. 2008, *A&A*, 483, 949
Lepreti, F., Carbone, V., Abramenko, V. I., and 4 coauthors, 2012, *ApJ* (Letters), 759, L17
Monin, A. S. & Yaglom, A. M. 1975, *Statistical Fluid Mechanics*, ed. J.Lumley (MIT Press, Cambridge, MA)
Scherrer, P. H., Schou, J., Bush, R. I., and 10 co-authors. 2012, *Solar Phys*, 275, 207
Utz, D., Hanslmeier, A., Muller, R., Veronig, A., Rybak, J., & Muthsam, H. 2010, *A&A*, 511, A39
Yeates, A. R., Nandy, D., & Mackay, D. H. 2008, *ApJ*, 673, 544